Catalysis Today 160 (2011) 3–10

Contents lists available at ScienceDirect

Catalysis Today

journal homepage: www.elsevier.com/locate/cattod

Review

Gold-based catalysts for the water–gas shift reaction: Active sites and reaction mechanism☆

José A. Rodriguez*

Chemistry Department, Brookhaven National Laboratory, Chemistry 555 Upton, NY 11973, USA

ARTICLE INFO

Article history:
Available online 29 July 2010

Keywords:
Gold
Ceria
Titania
Carbon monoxide
Hydrogen production
Water
Water–gas shift
CO oxidation

ABSTRACT

The water–gas shift (WGS, $CO + H_2O \rightarrow H_2 + CO_2$) reaction was studied on a series of gold/oxide catalysts. The results of *in situ* measurements with X-ray absorption spectroscopy indicate that the active phase of Au-ceria and Au-titania catalysts under the reaction conditions of the water–gas shift consists of metallic nanoparticles of gold on a partially reduced oxide support. In spite of the lack of catalytic activity of Au (1 1 1) and other gold surfaces for the water–gas shift process, gold nanoparticles dispersed on oxide surfaces are excellent catalysts for this reaction. Results of density-functional calculations point to a very high barrier for the dissociation of H_2O on Au (1 1 1) or isolated Au nanoparticles, which leads to negligible activity for the WGS process. In the gold-oxide systems, one has a bifunctional catalyst: the adsorption and dissociation of water takes place on the oxide, CO adsorbs on the gold nanoparticles, and all subsequent reaction steps occur at oxide–metal interfaces. The nature of the support plays a key role in the activation of the gold nanoparticles. Although zinc oxide is frequently used in industrial WGS catalysts, the Au/ZnO (0 0 0 $\bar{1}$) system displays low WGS activity when compared to Au/CeO_2 (1 1 1), Au/TiO_2 (1 1 0) or $Au/CeO_x/TiO_2$ (1 1 0). The ceria and titania supports contain a substantial number of metal cations that are not fully oxidized under WGS reaction conditions and may participate directly in the dissociation of water and other important steps of the catalytic process. The results for $Au/CeO_x/TiO_2$ (1 1 0) illustrate the tremendous impact that an optimization of the chemical properties of gold and the oxide phase can have on the activity of a WGS catalyst.

Contents

1. Introduction 3
2. The water–gas shift reaction on gold-ceria powder catalysts: *in situ* characterization with X-ray absorption spectroscopy 4
3. Water–gas shift reaction on Au nanoparticles supported on well-defined surfaces of oxides 5
4. Water–gas shift reaction on Au (1 1 1) and CeO_x/Au (1 1 1) surfaces 6
5. Water–gas shift reactions on $Au/CeO_x/TiO_2$ (1 1 0) surfaces 8
6. Conclusions 10
Acknowledgements 10
References 10

1. Introduction

This article reviews a series of studies examining the water–gas shift activity of gold-based catalysts. Currently, the primary source of hydrogen for the chemical and petrochemical industries comes from the steam reforming of hydrocarbons: $C_nH_m + nH_2O \rightarrow nCO + (n - m/2)\ H_2$ [1]. The reformed fuel usually contains 1–10% of CO, an impurity that can be a serious problem for chemical processes, which use H_2 as a feedstock. The water–gas shift reaction (WGS, $CO + H_2O \rightarrow H_2 + CO_2$) is critical for providing clean hydrogen [1,2]. Common industrial catalysts for the WGS (mixtures of Fe–Cr or Zn–Al–Cu oxides) are pyrophoric and normally require lengthy and complex activation steps before usage [1]. Recent works report that Au nanoparticles supported on oxides such as CeO_2 and TiO_2 are very efficient catalysts for the WGS reaction [2–5]. This is remarkable since neither bulk Au nor bulk ceria and titania are known as WGS catalysts.

Bulk metallic gold typically exhibits a very low chemical and catalytic activity [1,6]. Among the transition metals, gold is by far the least reactive [6], and is often referred to as the "coinage

☆ This paper is for a special issue entitled "Heterogeneous Catalysis by Metals: New Synthetic Methods and Characterization Techniques for High Reactivity" guest edited by Jinlong Gong and Robert Rioux.

* Tel.: +1 631 344 2246; fax: +1 631 344 5815.
E-mail address: rodrigez@bnl.gov.

0920-5861/$ – see front matter © 2010 Elsevier B.V. All rights reserved.
doi:10.1016/j.cattod.2010.06.030

metal". In the last 10 years, gold has become the subject of a lot of attention due to its unusual catalytic properties when dispersed on some oxide supports [7–17]. Several models have been proposed for explaining the activation of supported gold: from special chemical properties resulting from the limited size of the active gold particles (usually less than 10 nm), to the effects of metal ↔ support interactions (i.e. charge transfer between the oxide and gold) [4,5,7–9,12–14,17]. In principle, the active sites for the catalytic reactions could be located only on the supported Au particles or on the perimeter of the gold-oxide interface [4,5,7,12,17].

The nature of the active phase(s) in these metal/oxide WGS catalysts and the WGS reaction mechanism are still unclear. For example, the as prepared Au–CeO_2 catalysts contain nanoparticles of pure gold and gold oxides (AuO_x) dispersed on a nanoceria support [3]. Each of these gold species could be in the active phase [3,5] and the ceria support may not be a simple spectator in these systems [15,18]. Although pure ceria is a very poor WGS catalyst, the properties of this oxide were found to be crucial for the observed activity of the Au–CeO_2 nanocatalysts [2,3,19]. Several studies dealing with metal/oxide powder catalysts and the WGS indicate that the oxide plays a direct role in the reaction [2,3,5,18,20,21], but because of the complex nature of these systems, there is no agreement on its role. Results of density–functional calculations point to a very high barrier for the dissociation of H_2O on Au (1 1 1) or Au (1 0 0) [22], which leads to negligible activity for the WGS process. Even gold nanoparticles cannot dissociate water and catalyze the WGS [22]. Furthermore, surfaces and nanoparticles of copper are by far much better catalysts for the WGS than surfaces and nanoparticles of gold [22]. Thus, how can Au/CeO_2 catalysts be much more active than conventional Cu/ZnO catalysts?

In this article, we discuss recent published studies investigating the behavior of gold-oxide WGS catalysts. First, we will focus on the *in situ* characterization of gold-ceria powder catalysts using X-ray absorption spectroscopy [5,10,23]. This will be followed by a review of studies that investigate the properties of model WGS catalysts generated by the deposition of Au nanoparticles on well-defined surfaces of several oxides (CeO_2, TiO_2, MoO_2, ZnO, MgO) [4,10,25]. Then, we will present mechanistic studies for the WGS on Au (1 1 1) and inverse CeO_x/Au (1 1 1) catalysts [26–28]. The article ends with a discussion of the properties of a novel and extremely active Au/CeO_x/TiO_2 (1 1 0) catalyst, which takes advantage of the special properties of gold and ceria nanoparticles supported on a titania support [29,30].

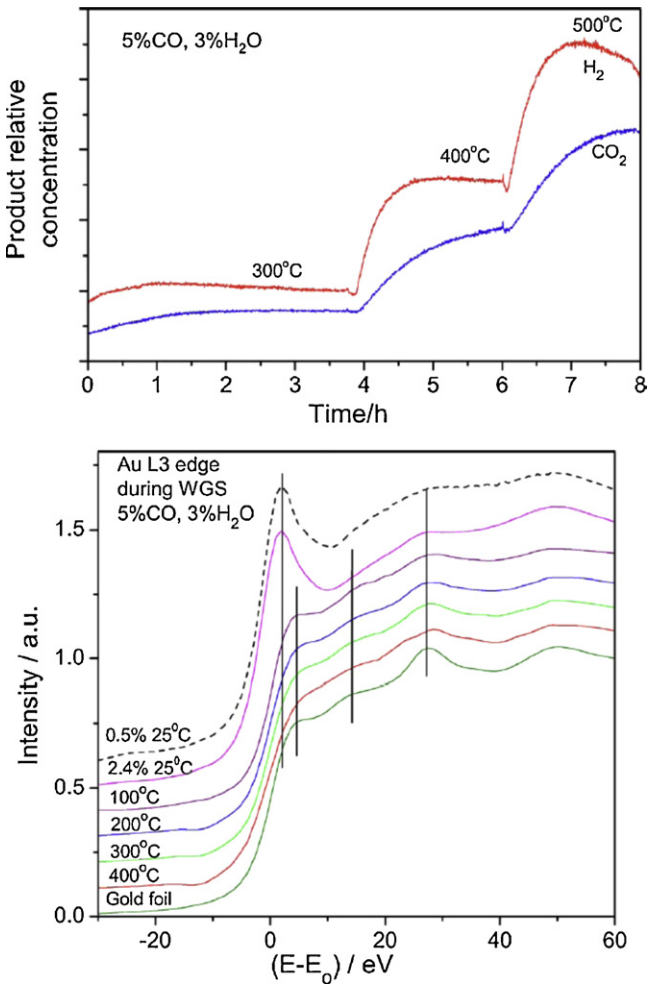

Fig. 1. Top panel: relative amounts of H_2 and CO_2 formed during the WGS over a 2.4 wt% Au-ceria catalysts. A mixture of 5% CO and 3% H_2O in He (total flow ~10 ml/min) was passed over the catalyst at 300, 400, or 500 °C [10,23]. Bottom panel: Au L_3-edge XANES spectra collected *in situ* during the WGS reaction over the 2.4 wt% Au–CeO_2 catalyst. For comparison, we also include the spectra for a fresh 0.5 wt% Au–CeO_2 catalyst, dashed trace, and a gold foil. The vertical lines indicate the main features for AuO_x versus metallic Au.

2. The water–gas shift reaction on gold-ceria powder catalysts: *in situ* characterization with X-ray absorption spectroscopy

Originally, it was suggested that the active phase in Au–CeO_2 catalysts are AuO_x nanoparticles or more specifically cationic $Au^{\delta+}$ species [3]. The top panel in Fig. 1 shows data for the production of H_2 and CO_2 during the WGS over a powder gold-ceria catalyst [10]. The catalyst was held at temperatures of 300, 400 and 500 °C. The experimental set-up did not detect significant catalytic activity at temperatures below 250 °C [10]. The chemical state of gold during the WGS was determined by means of *in situ* time-resolved X-ray absorption near-edge spectroscopy (XANES). The bottom panel in Fig. 1 displays Au L_3-edge XANES spectra collected at room temperature for fresh catalysts with a Au content of 0.5 wt% (dashed trace) or 2.4 wt% (solid traces) [10]. The line-shape of these two spectra is very similar and shows a clear feature at ~2.5 eV above the edge that is not seen for metallic gold and is characteristic of gold oxides [10,31]. The intensity of this peak is higher than that observed for Au_2O and closer to that seen in Au_2O_3 [31]. Once the 2.4 wt% Au–CeO_2 catalyst was exposed to a mixture of CO/H_2O at elevated temperatures, the XANES features for gold oxide disappeared. At temperatures above 200 °C, when significant WGS activity was detected, the line-shape of the Au L_3-edge resembled that of pure gold. The XANES spectra in Fig. 1 were obtained under a reaction mixture of 5% CO and 3% H_2O in He (total flow ~10 ml/min) [10]. Similar results were found when using a 1% CO and 3% H_2O in He reaction mixture. Thus, the *in situ* time-resolved XAS data indicate that cationic $Au^{\delta+}$ species cannot be the key sites responsible for the WGS activity in Fig. 1, because they do not exist under reaction conditions [10]. An identical finding has been reported for $AuO_x/Ce_{1-x}Zr_xO_{2-y}$ powder catalysts [5]. In these catalysts, the active phase consisted of small Au aggregates (<2 nm in size) dispersed on partially reduced ceria ($CeO_{1.94}$–$CeO_{1.98}$) [5,10,23].

In another set of experiments, interfaces of AuO_x/CeO_2 were prepared by first vapor-depositing small amounts of Au (<0.2 ML) on a Ce film supported on Pt (1 1 1), with subsequent oxidation by reaction with 500 Torr of O_2 in a high-pressure cell [10]. This produced AuO_x/CeO_2 interfaces that had XPS spectra with the typical Ce 3d features of Ce^{4+} cations and Au $4f_{7/2}$ peaks located in between those expected for Au^{1+} and Au^{3+} cations. The gold oxide in the AuO_x/CeO_2 interfaces was fully reduced upon exposure to CO, H_2 or reaction mixtures that had a CO/H_2O ratio varying from 0.2 to 2

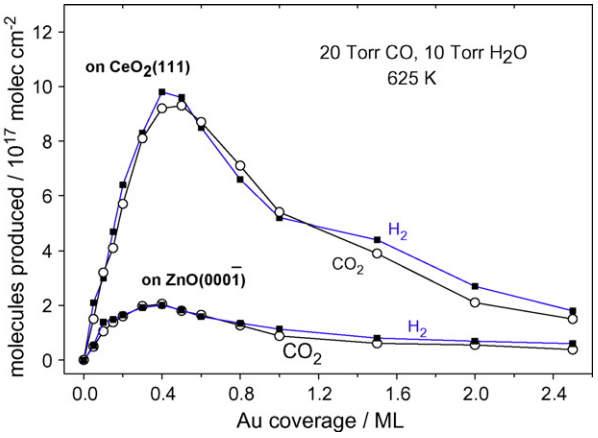

Fig. 2. WGS activity of model Au/CeO_2 (1 1 1) and Au/ZnO (0 0 0 $\bar{1}$) catalysts as a function of gold coverage. Each surface was exposed to a mixture of 20 Torr of CO and 10 Torr of H_2O at 625 K for 5 min. Steady-state was reached 2–3 min after introducing the gases in the batch reactor.

[10]. Thus, a $AuO_x \rightarrow Au$ transformation readily occurs in reducing environments.

3. Water–gas shift reaction on Au nanoparticles supported on well-defined surfaces of oxides

The kinetics of the WGS reaction have been investigated in detail on model catalysts generated by vapor-depositing nanoparticles of gold on CeO_2 (1 1 1) [4,10], ZnO (0 0 0 $\bar{1}$) [4], TiO_2 (1 1 0) [25] and polycrystalline MoO_2 [24]. On these oxide substrates, gold grows forming three-dimensional (3D) particles [4,25,29]. Fig. 2 displays the behavior of the Au/CeO_2 (1 1 1) and Au/ZnO (0 0 0 $\bar{1}$) catalysts as a function of gold coverage [4]. CeO_2 (1 1 1) and ZnO (0 0 0 $\bar{1}$) are both O terminated surfaces. These oxide supports are inactive as catalysts for the WGS reaction. In Fig. 2, the catalytic activity of the metal/oxide systems initially increases when Au is added, reaching a maximun at ~0.4–0.5 monolayer (ML). Above these coverages, the overall catalytic activity decreases. Similar trends have been observed for the WGS on Au/TiO_2 (1 1 0) [25] and Au/MoO_2 [24]. STM images show that the particle size of Au on CeO_2 (1 1 1), ZnO (0 0 0 $\bar{1}$) or TiO_2 (1 1 0) raises above 4 nm and continuously grows when the admetal coverage is increased beyond 0.5 ML [4,25,29]. The trends in Fig. 2 probably reflect changes in the size of the gold particles: High catalytic activity is seen for small gold particles (size <4 nm), and it decreases as the particle size increases. Although the optimum WGS activity in Fig. 2 is for admetal coverages of 0.4–0.5 ML, metal/oxide catalysts with gold coverages near 1 ML are still substantially more active than Au (1 1 1) or polycrystalline gold, surfaces which are not catalytically active [4].

The gold atoms in the Au/CeO_2 (1 1 1) and Au/ZnO (0 0 0 $\bar{1}$) catalysts were probably not oxidized during the WGS process [4]. After reaction, XPS showed Au 4f positions that were almost identical to those seen upon deposition of gold on the oxides and very different from those typical seen for AuO_x species [4,10]. Post-reaction surface analysis also showed the presence of formate- and/or carbonate-like groups on the surface of the catalysts. Possible reaction paths for the formation of these groups are discussed in Ref. [5]. It is not completely clear if they are key intermediates in the WGS process or simple spectators [4,5,25].

The top panel in Fig. 3 compares the WGS activity of Au (1 1 1) and 0.5 ML of Au supported on ZnO (0 0 0 $\bar{1}$) [4], CeO_2 (1 1 1) [4] and a MoO_2 film [24]. The nature of the support plays a key role in the activation of the gold nanoparticles. Zinc oxide is frequently used in industrial Cu–ZnO WGS catalysts [1]. However, the Au/ZnO (0 0 0 $\bar{1}$) system displays low WGS activity when compared to Au/CeO_2

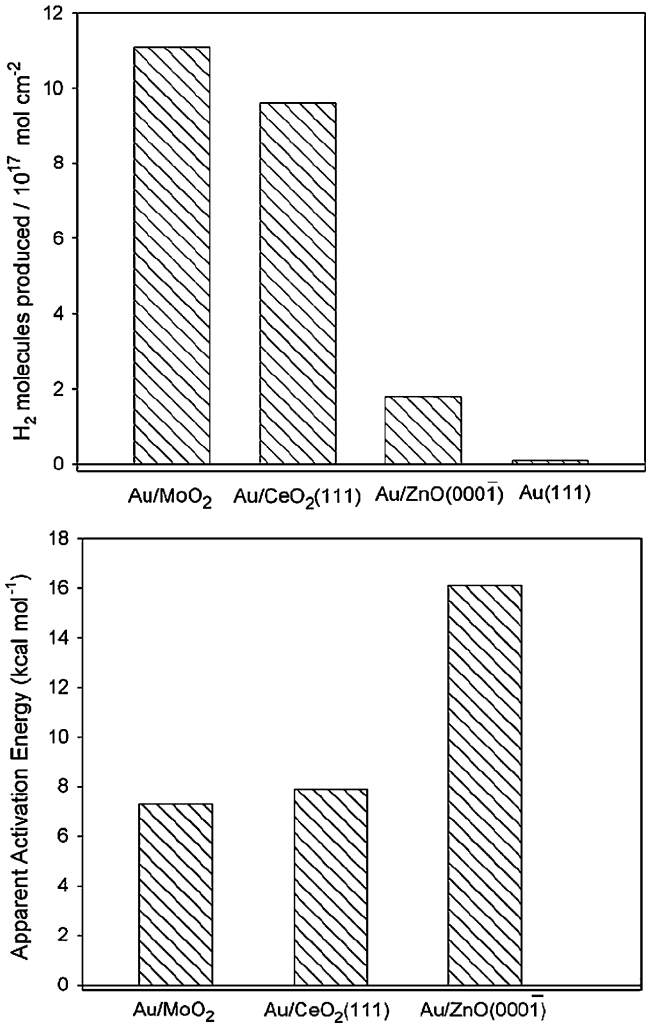

Fig. 3. Top panel: WGS activity of Au (1 1 1) and 0.5 ML of Au supported on ZnO (0 0 0 $\bar{1}$) [4], CeO_2 (1 1 1) [4,10] and polycrystalline MoO_2 [24] (20 Torr of CO and 10 Torr of H_2O at 625 K for 5 min). Bottom panel: apparent activation energies observed for the WGS over 0.5 ML of Au dispersed on ZnO (0 0 0 $\bar{1}$) [4], CeO_2 (1 1 1) [4,10] and polycrystalline MoO_2 [24] (20 Torr of CO and 10 Torr of H_2O).

(1 1 1) [4], Au/MoO_2 [24] or Au/TiO_2 (1 1 0) [25]. The ceria, molybdena and titania contain a substantial number of metal cations that are not fully oxidized under WGS reaction conditions and may participate directly in important steps of the process [4,24,25]. This is not the case for Au/ZnO (0 0 0 $\bar{1}$) [4].

The bottom panel in Fig. 3 displays the apparent activation energies observed for 0.5 ML of Au deposited on ZnO (0 0 0 $\bar{1}$) [4], CeO_2 (1 1 1) [4] and MoO_2 [24]. All the reported values were obtained from Arrhenius plots that contained reaction rates measured at 575, 600, 625 and 650 K under steady state conditions at P_{CO} = 20 Torr and P_{H_2O} = 10 Torr. The more active catalysts have apparent activation energies in the range of 7–8.5 kcal/mol, while the corresponding value for the less active catalysts is ~16 kcal/mol. The presence of O vacancies in the CeO_2 (1 1 1) and MoO_2 substrates facilitates the dissociation of water and, thus, probably leads to a relatively low apparent activation energy for the WGS [4,24].

Copper-based WGS catalysts are quite common in industrial applications, in particular the Cu/ZnO system [1,5]. Fig. 4 compares the WGS activity of 0.5 ML of Au and Cu deposited on CeO_2 (1 1 1) and ZnO (0 0 0 $\bar{1}$) with the corresponding activity of Au (1 1 1) and Cu (1 0 0) [4]. The WGS activity seen for Cu (1 0 0) is in between that detected for Cu (1 1 1) and Cu (1 1 0) [32,33]. The deposition of Cu nanoparticles on ZnO (0 0 0 $\bar{1}$) produces a catalyst that is clearly

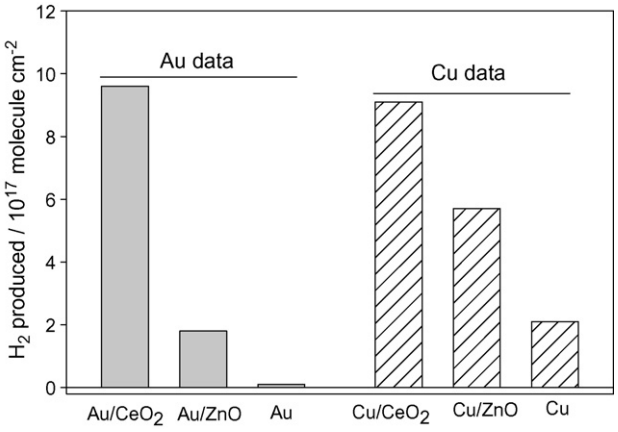

Fig. 4. Amounts of H_2 produced during the WGS reaction on 0.5 ML of gold or copper deposited on CeO_2 (1 1 1) [4,10] and ZnO (0 0 0 $\bar{1}$) [4]. For comparison are also included the activities of Au (1 1 1) and Cu (1 0 0) [4,10]. The catalysts were exposed to a mixture of 20 Torr of CO and 10 Torr of H_2O at 625 K for 5 min in a batch reactor [4,10,24]. A reaction time of 2–3 min was enough to reach a steady-state regime in the reactor.

more active than the pure extended Cu surfaces [4]. An even better catalyst is obtained when the Cu nanoparticles are supported on CeO_2 (1 1 1). The Au/ZnO (0 0 0 $\bar{1}$) system displayed a catalytic activity worse than that of Cu/ZnO (0 0 0 $\bar{1}$). On the other hand, Au/CeO_2 (1 1 1) is an excellent catalyst with an activity similar to that of Cu/CeO_2 (1 1 1) [4]. The next section analyzes the causes behind the dramatic effects that ceria has on the WGS activity of gold.

4. Water–gas shift reaction on Au (1 1 1) and CeO_x/Au (1 1 1) surfaces

Why are extended surfaces of gold inactive as catalysts for the WGS reaction? Fig. 5 shows the calculated energy profile for the WGS on periodic Cu (1 0 0) and Au (1 0 0) surfaces [22]. On Cu (1 0 0), the first and the most energy-consuming step, or rate-limiting step, is water dissociation with a ΔE_3 of +0.39 eV and a barrier (ΔEa_3) of +1.13 eV. The cleavage of the first O–H bond is also the rate-limiting step on a Cu (1 1 0) surface [33]. In contrast, the dissociation of adsorbed OH* and the formation of CO_2 are more facile. All the

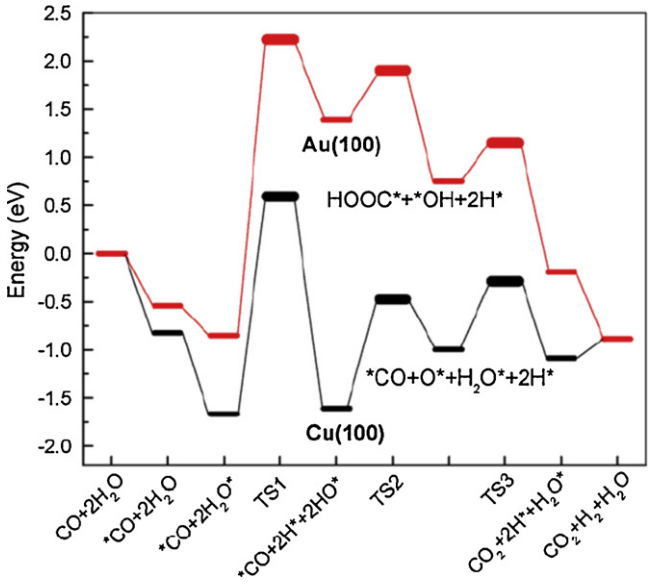

Fig. 5. DFT calculated [18,22] reaction profile for the WGS on Cu (1 0 0) and Au (1 0 0).

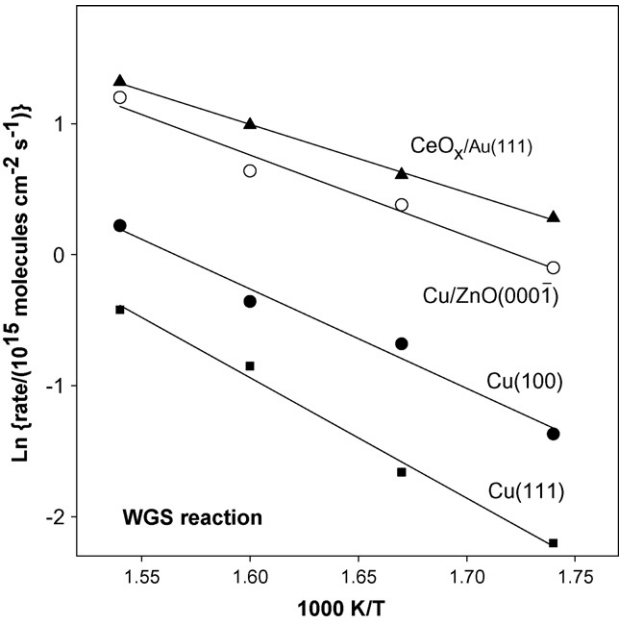

Fig. 6. Arrhenius plot for the WGS reaction rate on Cu (1 1 1) [36], Cu (1 0 0) [4], Cu/ZnO (0 0 0 $\bar{1}$) [4] and on a Au (1 1 1) surface approximately 20% covered by.ceria [18,27]. The data were acquired with a pressure of 20 Torr of CO and 10 Torr of H_2O and temperatures of 575, 600, 625 and 650 K.

adsorbates bond more weakly on Au (1 0 0) than on Cu (1 0 0). Consequently, the rate-limiting dissociation of H_2O on Au (1 0 0) is even more endothermic (ΔE_3 = +0.74 eV) and the corresponding barrier is also higher (ΔEa_3 = +1.53 eV). These DFT results are in agreement with experimental measurements, which show that Cu is a good WGS catalyst while Au is an extremely poor one [4,32,33]. The results in Fig. 5 indicate that gold will be an excellent WGS catalyst if in some way is helped with the dissociation of water [22]. Assuming that OH can be formed on Au (1 0 0) or Au (1 1 1), subsequent steps for the WGS process should occur readily on the gold substrate [22]. Indeed, experimental and theoretical studies have shown that water dissociates on O/Au (1 1 1) yielding hydroxyls which react with CO to produce CO_2 and hydrogen [34,35].

One can obtain a stable catalyst for the WGS by adding CeO_x nanoparticles to Au (1 1 1) [18,27]. Fig. 6 displays an Arrhenius plot for the WGS activity of a CeO_x/Au (1 1 1) surface in which 20% of the gold substrate was covered by ceria [27]. For comparison we also include results obtained for the WGS on Cu (1 0 0) [4], Cu (1 1 1) [36] and Cu/ZnO (0 0 0 $\bar{1}$) [4] surfaces. The results in Fig. 6 indicate that the inverse CeO_x/Au (1 1 1) catalyst exhibits a larger WGS activity than those of copper surfaces or even Cu nanoparticles dispersed on a ZnO (0 0 0 $\bar{1}$) substrate. On Cu (1 1 1) and Cu (1 0 0), the apparent activation energies for the WGS are 18.1 and 15.2 kcal/mol, respectively [4,36]. The apparent activation energy decreases to 12.4 kcal/mol on Cu/ZnO (0 0 0 $\bar{1}$) [4] and 10.3 kcal/mol on CeO_x/Au (1 1 1) [27]. In the inverse CeO_x/Au (1 1 1) catalyst, the reactants can interact with defect sites of ceria nanoparticles, metal sites of the support, or the metal–oxide interface [27,28]. One can gain activity due to the active participation of oxide in the catalytic reaction [28].

Post-reaction characterization of the inverse CeO_x/Au (1 1 1) catalyst with XPS pointed to a $Ce^{4+} \rightarrow Ce^{3+}$ transformation and identified a C 1s feature at 289–290 eV corresponding to either HCOO or CO_3 species on the CeO_x/Au (1 1 1) surface [18,27]. The mechanism for the WGS in CeO_x/Au (1 1 1) is assumed to undergo the following pathway [18]:

$$CO \rightarrow CO(a)$$

$$H_2O \rightarrow H_2O(a)$$

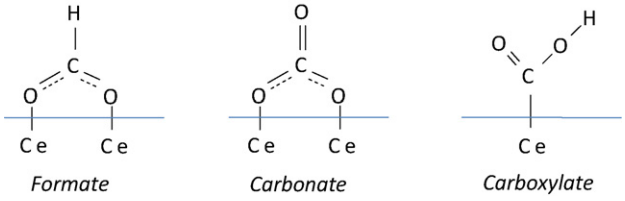

Fig. 7. Different coordination modes for formate (HCOO), carbonate (CO_3) and carboxylate (HOCO) on a nanoparticle or surface of ceria.

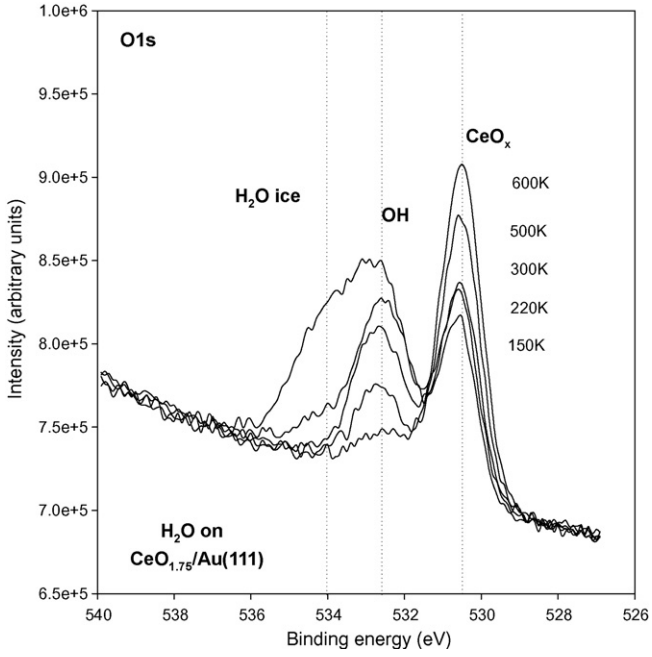

Fig. 8. XPS spectra in the O 1s region for a dose of 2.3 L of H_2O to $CeO_{1.75}$/Au (1 1 1) followed by annealing steps as depicted from 150 to 600 K.

$$H_2O(a) \rightarrow OH(a) + H(a)$$

$$CO(a) + OH(a) \rightarrow HCO_x(a)$$

$$HCO_x(a) \rightarrow CO_2 + H(a)$$

$$2H(a) \rightarrow H_2$$

A stable HCO_x intermediate species must precede the formation of H_2 and CO_2. It has been proposed that the key intermediate species for the WGS reaction is either a formate (HCOO) or a carbonate (CO_3) [1,5]. Recent theoretical calculations also suggest the possibility of a carboxylate (HOCO) intermediate [22,37]. These species have different coordination modes (see Fig. 7) and different life-times on the surface of the catalyst.

Adsorption of HCOOH and CO_2 was used to create HCOO and CO_3 groups on CeO_x/Au (1 1 1) surfaces [27]. The orientation of the formate on the ceria nanoparticles supported on Au (1 1 1) is likely to be near normal to the surface as a bidentate species in a chelating or bridged conformation. No preferred orientation was observed for adsorbed carbonate [27]. $HCOO_{ads}$ appeared to have greater stability than $CO_{3,ads}$ with desorption temperatures up to 600 K while CO_3 only survived on the surface up to 300 K. Both species could be valid intermediates for the WGS because the reaction temperatures in Fig. 6 are elevated (575–650 K) [27].

On the CeO_x/Au (1 1 1) catalysts, the presence of Ce^{3+} led to the dissociation of H_2O to give OH groups [18,27]. Fig. 8 displays O 1s

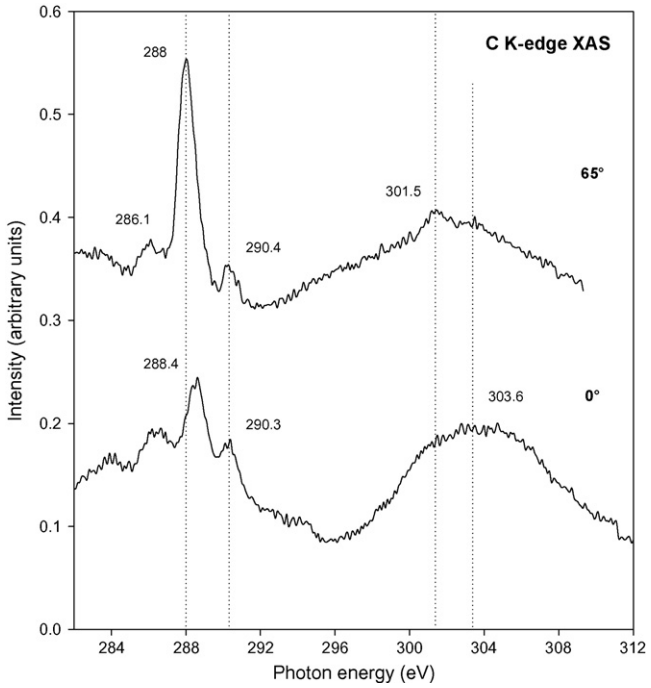

Fig. 9. C K-edge NEXAFS of CO (3 L) dosed to hydroxylated $CeO_{1.75}$/Au (1 1 1) at 100 K. Both the normal incidence (0°) angle and the grazing incidence (65°) spectra are shown in the figure.

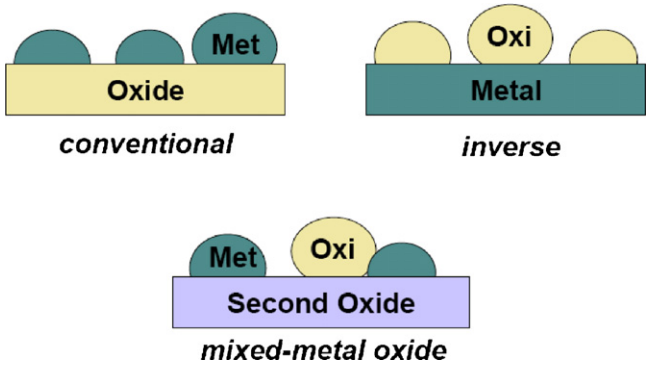

Fig. 10. Different configurations for a metal–oxide catalyst.

spectra collected after adsorbing H_2O on a $CeO_{1.75}$/Au (1 1 1) surface at 100 K with subsequent annealing to the indicated temperatures. These data indicate that OH species are stable on the surface up to 600 K and could interact with CO to yield weakly bound intermediates. When there is an abundance of Ce^{4+}, the OH concentration is diminished and the likely intermediates are carbonates [27]. As the surface defects are increased and the Ce^{3+}/Ce^{4+} ratio grows, the OH concentration also grows and both carbonate and formate species are observed on the surface after dosing CO to H_2O/CeO_x/Au (1 1 1) [27]. Fig. 9 shows data for the exposure of 3 L of CO onto a heavily hydroxylated CeO_x/Au (1 1 1) surface that had a large Ce^{3+} concentration. This set of C K-edge data is complex with many contributions evident [27]. The peaks that appear at 288 and 288.4 eV share close resemblance to that of the $\pi^*C{=}O$ resonance the grazing and normal incidence for formates. The 290.4 and 290.3 eV peaks are close to the $\pi^*C{-}O$ resonance of carbonates in grazing and normal incidences. The peak at 286.1 eV is due to CO adsorbed on the surface. Weaker, broader contributions at 301.5 and 303.6 eV are likely a mixture of σ features from both $CO_{3,ads}$ and formate $HCOO_{ads}$ species [27]. The data, however, do not contain the features expected for an adsorbed carboxylate (HOCO) intermediate [26,27].

A possible scenario for reaction of CO with OH in presence of O is [27]:

$[Ce^{4+}]$

$$2CO + 0.5OH_{ads} + 2O_{ads} \rightarrow CO_{ads} + CO_{3,ads} + 0.5OH_{ads}$$

$$CO_{ads} + CO_{3,ads} + 0.5OH_{ads} \rightarrow 2CO_2 + 0.25H_2 + 0.5O_{ads}$$

$[Ce^{3+}/Ce^{4+}]$

$$2CO + OH_{ads} + O_{ads} \rightarrow 0.5CO_{3,ads} + HCO_{2,ads} + 0.5CO_{ads}$$

$$0.5CO_{3,ads} + HCO_{2,ads} + 0.5CO_{ads} \rightarrow 2CO_2 + 0.5H_2$$

The ratio of OH:O (oxide) on the surface dictates the chemical specificity of the intermediate that arises [27]. The addition of ceria nanoparticles to Au (1 1 1) is essential to generate an active WGS catalyst and to increase the production and stability of key reaction intermediates (OH, HCOO and CO_3). The Ce^{3+} is critical to OH formation and a likely scenario may be that the OH could spill over from the CeO_x nanoparticles on to the Au (1 1 1) surface [18,27]. The carboxylate (HOCO) intermediate seen in DFT calculations [22,37] is experimentally elusive and difficult to detect [27]. The low thermal stability of the carboxylate makes it an ideal transient species for the WGS [18,22,25,37] and it may only be observed under steady state conditions.

5. Water–gas shift reactions on $Au/CeO_x/TiO_2$ (1 1 0) surfaces

The studies described above indicate that highly active WGS catalysts are bifunctional with the metal and oxide catalyzing different parts of the reaction. To optimize the performance of these systems one must enhance the participation of the metal and oxide phases in the catalytic process. Fig. 10 shows three different configurations in which a metal and an oxide can be combined in a catalyst. In a conventional metal/oxide configuration, one enhances the reactivity of the metal but this usually covers the defect sites of the oxide (nucleation centers for the metal particles), which have chemical activity. This is not the case in the inverse oxide/metal catalyst,

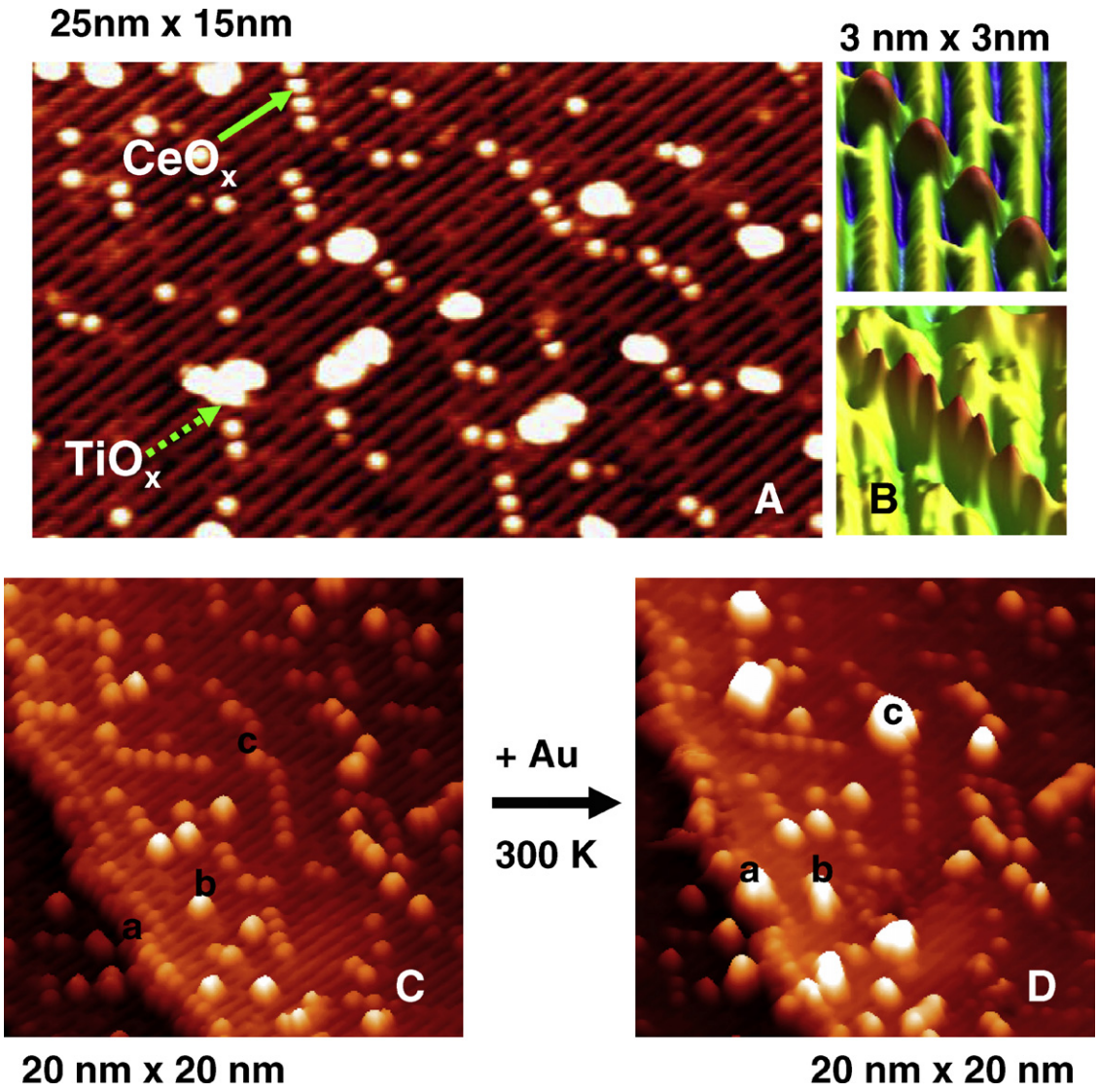

Fig. 11. (A) STM image of CeO_x on the TiO_2 (1 1 0) surface after depositing Ce atoms at 600 K in O_2 (P_{O_2} : 1×10^{-7} Torr) and subsequent annealing at 900 K in O_2 (P_{O_2} : 1×10^{-4} Torr), V_t: 1.2 V, I_t: 0.07 nA) [29]. (B) Bias dependent STM images of a diagonal array of CeO_x nanoparticles taken at the imaging bias of 1.2 V, 0.06 nA (top) and 0.4 V, 0.06 nA (bottom). (C) STM image of a CeO_x/TiO_2(1 1 0) surface. As in part A, Ce was deposited at 600 K under an atmosphere of O_2 ($\sim 1 \times 10^{-7}$ Torr) and then the sample was annealed at 900 K in O_2 [29]. (D) STM image for a $Au/CeO_x/TiO_2$ (1 1 0) surface. The gold was deposited on the same area shown in "B" at ~300 K. ~6% of the surface was covered with Au. Imaging conditions of V_t = 1.5 V and I_t = 0.03 nA for parts (C) and (D).

which enhances the participation of the oxide in the catalytic reaction [28]. In the inverse catalyst, the reactants can interact with defect sites of oxide nanoparticles, metal sites of the support, or the metal–oxide interface [28]. In the quest to optimize the reactivity of the metal and oxide phases, the most complex and promising configuration is a mixed-metal oxide array in which nanoparticles of a metal and an oxide can interact with the reactants. Extremely active WGS catalysts have been found after coadsorbing nanoparticles of gold and ceria on a TiO_2 (1 1 0) substrate [29].

In recent years there has been a strong interest in obtaining a fundamental understanding of the behavior of mixed-metal oxide catalysts [38]. In principle, the combination of two metals in an oxide matrix can produce materials with novel structural or electronic properties that can lead to superior catalytic activity or selectivity [38–41]. The deposition of Ce atoms or CeO_x clusters on a TiO_2 (1 1 0) substrate produces structures which are very different from those of bulk ceria or ceria nanoparticles supported on metal surfaces or silica films [29,38]. Panel A in Fig. 11 shows a STM image obtained after depositing Ce on the TiO_2 (1 1 0) surface at 600 K in O_2 ($\sim 1 \times 10{-}7$ Torr) and the sample was subsequently annealed to 900 K still under an O_2 environment [29]. The image was taken after cooling the sample down to room temperature and removing the O_2 from the background. Two different types of features are observed on the terraces: diagonal arrays of small bright spots (see solid arrow) and bigger ones (see dashed green arrow). The bigger clusters in Fig. 11A can be correlated with TiO_x islands (~3 Å in height), which resulted from reaction of oxygen gas with interstitial Ti from the reduced bulk [29]. The diagonal arrays (see solid arrow) have a distinctive height (1.4 Å) and correspond to CeO_x nanoparticles [29]. To better understand the structures of the CeO_x nanoparticles, a bias dependent STM measurement was performed as shown in Fig. 11B. These two images display the same diagonal arrays of CeO_x nanoparticles, but obtained at different imaging bias. The top STM image was taken with an imaging bias of +1.2 V and the angle of the diagonal array is close to 42° with respect to the [1–10] direction. When this feature was imaged at +0.4 V, the individual bright features appeared as dimmers [29]. Each ceria dimer is located in between two rows of oxygens protruding from the surface. XPS and UPS spectra indicated that the oxidation state of the Ce atoms in the dimers was essentially 3+ [29,42]. The titanium cations were mainly Ti^{4+} with a small amount (<5%) of Ti^{3+} comparable to that found on clean TiO_2 (1 1 0) [29,42].

CeO_x nanoparticles drastically affect the growth mode of Au on TiO_2 (1 1 0) [29]. On this surface, the admetals grow forming three-dimensional particles. Gold exhibits very weak interactions with the ideal terraces of TiO_2 (1 1 0) [25] and mainly binds to defects or step sites [29,43]. Fig. 11 displays STM images acquired from the same surface area before (part C) and after (part D) depositing gold on CeO_x/TiO_2 (1 1 0) at ~300 K [29]. The CeO_x/TiO_2 (1 1 0) was pre-annealed under O_2 ($\sim 1 \times 10^{-7}$ Torr) at 900 K and had a morphology similar to that seen in Fig. 11A. The deposition of Au at room temperature, ~0.2 ML, produced three-dimensional metal particles anchored to steps of the titania surface, "a" sites, to the (1×2) reconstructions of TiO_2 (1 1 0), "b" sites, and to the CeO_x dimers, "c" sites [29]. On CeO_x/TiO_2 (1 1 0), the dispersion of the Au was substantially larger than seen on a pure TiO_2 (1 1 0) surface where Au mainly binds to the steps [29,43].

Neither CeO_x/TiO_2 (1 1 0) nor Au (1 1 1) are able to catalyze the WGS [4,29]. However, $Au/CeO_x/TiO_2$ (1 1 0) surfaces are outstanding catalysts for the WGS as shown in Fig. 12. In test experiments, Au/TiO_2 (1 1 0) surfaces were prepared following the same steps used for the synthesis of $Au/CeO_x/TiO_2$ (1 1 0) but without the deposition of cerium [29]. The Au/TiO_2 (1 1 0) systems were good WGS catalysts, see top panel in Fig. 12, but they did not come close to match the activity of $Au/CeO_x/TiO_2$ (1 1 0) [29]. The same is valid when comparing to the WGS activities of Au/CeO_2 (1 1 1) [4], CeO_x/Au (1 1 1) [18,27], Cu/ZnO (0 0 0 $\bar{1}$) [4], and copper single crystals [4,21,36]. As mentioned above, Cu/ZnO is the most common WGS catalyst used in the industry [1] and copper is the best pure metal catalyst [4,21,36,37,44]. For the $Au/CeO_x/TiO_2$ (1 1 0) catalyst in Fig. 12, one could assume that the concentration of active sites is proportional to the number of ceria regions in contact with gold nanoparticles [29]. Since only 12% of the titania support was covered by ceria, as measured by ion scattering spectroscopy (ISS), the $Au/CeO_x/TiO_2$ (1 1 0) catalyst must be at least 300 times more active than a Cu (1 0 0) surface on a per active-site basis [29].

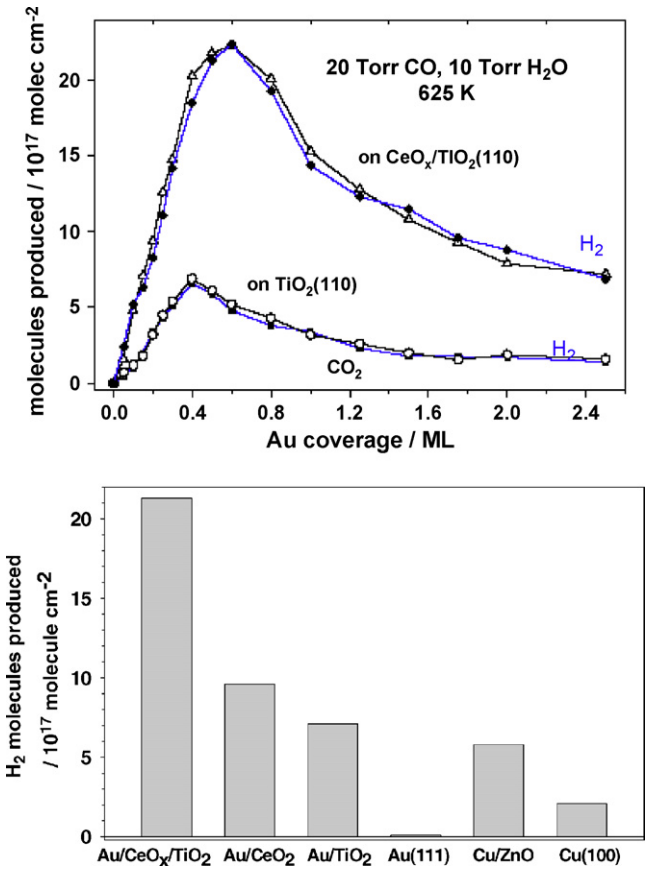

Fig. 12. Top panel: Water–gas shift activity of Au/TiO_2 (1 1 0) [25] and $Au/CeO_x/TiO_2$ (1 1 0) [29] as a function of Au coverage. The area of TiO_2 (1 1 0) covered by CeO_x was measured with ISS, before depositing gold, and found to be ~12% of the clean substrate [29]. The reported values for the production of H_2 (blue curve) and CO_2 (black curve) were obtained after exposing the catalysts to 20 Torr of CO and 10 Torr of H_2O at 625 K for 5 min [25,29]. The number of H_2 and CO_2 molecules produced is normalized by the sample surface area. Bottom panel: Comparison of the water–gas shift activity of Cu (1 0 0) [4], Au (1 1 1) [4], and 0.5 ML of Au supported on TiO_2 (1 1 0) [25], CeO_2 (1 1 1) [4] or CeO_x/TiO_2 (1 1 0) [29] (For interpretation of the references to color in this figure legend, the reader is referred to the web version of the article.).

The large dispersion of gold on CeO_x/TiO_2 (1 1 0), Fig. 11D, should lead to a high catalytic activity. The Ce^{3+} sites present in CeO_x/TiO_2 (1 1 0) easily dissociate water [42] but, upon exposure to CO, highly stable HCO_x species were formed on the oxide surface and there was no production of H_2 or CO_2 gas [29,42]. In $Au/CeO_x/TiO_2$ (1 1 0), one has a bifunctional catalyst: the adsorption and dissociation of water takes place on the oxide, CO adsorbs on the gold nanoparticles, and all subsequent reaction steps occur at oxide-metal interfaces. Au nanoparticles do catalyze the reaction of OH with CO to yield a HOCO intermediate and then H_2 and CO_2 [22,25]. The results in Fig. 12 illustrate the tremendous impact that an optimization of the chemical properties of gold and ceria can have on the activity of a WGS catalyst [29].

6. Conclusions

The active phase of Au-ceria and Au-titania catalysts under the reaction conditions of the water–gas shift consists of metallic nanoparticles of gold on a partially reduced oxide support. *In situ* experiments using X-ray absorption spectroscopy have shown that AuO_x species are not stable at elevated temperatures (>450 K) in the presence of CO, H_2 or CO/H_2O mixtures. In spite of the lack of catalytic activity of Au (1 1 1) and other gold surfaces for the water–gas shift process, gold nanoparticles dispersed on oxide surfaces are excellent catalysts for this reaction. Results of density–functional calculations point to a very high barrier for the dissociation of H_2O on Au (1 1 1) or isolated Au nanoparticles, which leads to negligible activity for the WGS process. In the gold-oxide systems, one has a bifunctional catalyst: The adsorption and dissociation of water takes place on the oxide, CO adsorbs on the gold nanoparticles, and all subsequent reaction steps occur at oxide-metal interfaces. Experimental evidence indicates that gold-oxide interfaces do catalyze the reaction of OH with CO to yield HCOO or CO_3 intermediates and then H_2 and CO_2.

The nature of the support plays a key role in the activation of the gold nanoparticles. Although zinc oxide is frequently used in industrial WGS catalysts, the Au/ZnO ($0\,0\,0\,\bar{1}$) system displays low WGS activity when compared to Au/CeO_2 (1 1 1), Au/MoO_2 or Au/TiO_2 (1 1 0). The ceria, molybdena and titania supports contain a substantial number of metal cations that are not fully oxidized under WGS reaction conditions and may participate directly in the dissociation of water and other important steps of the catalytic process. Extremely active WGS catalysts have been found after coadsorbing nanoparticles of gold and ceria on a TiO_2 (1 1 0) substrate. The $Au/CeO_x/TiO_2$ (1 1 0) system takes advantage of the complex interactions which occur in a mixed-metal oxide at the nanometer level, opening new directions for tuning catalytic activity by coupling appropriate pairs of oxides.

Acknowledgements

Many of the experiments described in the text of this article were done by the Group of Catalysis and Surface Science at Brookhaven National Laboratory (L. Barrio, M. Estrella, J.C. Hanson, J. Hrbek, P. Liu, S. Ma, A. Nambu, J.-B. Park, J.A. Rodriguez, S.D. Senanayake, D. Stacchiola, X. Wang, W. Wen) in collaboration with research groups at the Universidad Central de Venezuela (J. Evans, M. Pérez) and the Universidad de Sevilla (J. Graciani, J.F. Sanz). The research carried out at Brookhaven National Laboratory was supported by the US Department of Energy (Chemical Sciences Division, DE-AC02-98CH10886).

References

[1] J.M. Thomas, W.J. Thomas, Principles and Practice of Heterogeneous Catalysis, VCH, New York, 1997;
M.S. Spencer, Topics in Catalysis 8 (1999) 259.
[2] R. Si, M. Flytzani-Stephanopoulos, Angew. Chem. Int. Ed. 47 (2008) 2884.
[3] Q. Fu, H. Saltsburg, M. Flytzani-Stephanopoulos, Science 301 (2003) 935.
[4] J.A. Rodriguez, P. Liu, J. Hrbek, J. Evans, M. Pérez, Angew. Chem. Int. 46 (2007) 1329.
[5] R. Burch, Phys. Chem. Chem. Phys. 8 (2006) 5483.
[6] B. Hammer, J.K. Nørskov, Nature 376 (1995) 238.
[7] J.A. Rodriguez, Dekker Encyclopedia of Nanoscience and Nanotechnology, Dekker, New York, 2004, pp. 1297–1304.
[8] M. Haruta, Catal. Today 36 (1997) 153.
[9] M.S. Chen, D.W. Goodman, Science 306 (2004) 252.
[10] X. Wang, J.A. Rodriguez, J.C. Hanson, M. Perez, J. Evans, J. Chem. Phys. 123 (2005) 221101.
[11] J.A. Rodriguez, G. Liu, T. Jirsak, J. Hrbek, Z. Chang, J. Dvorak, A. Maiti, J. Am. Chem. Soc. 124 (2002) 5242.
[12] L.M. Molina, B. Hammer, Appl. Catal. A: Gen. 291 (2005) 21.
[13] H. Häkkinen, S. Abbet, A. Sanchez, U. Heiz, U. Landman, Angew. Chem. Int. Ed. 42 (2003) 1297.
[14] L. Giordano, G. Pacchioni, T. Bredow, J. Fernández-Sanz, Surf. Sci. 471 (2001) 21.
[15] J.A. Rodriguez, M. Pérez, J. Evans, G. Liu, J. Hrbek, J. Chem. Phys. 122 (2005) 241101.
[16] J.A. Rodriguez, M. Pérez, T. Jirsak, J. Evans, J. Hrbek, L. González, Chem. Phys. Lett. 378 (2003) 526.
[17] I.N. Remediakis, N. Lopez, J.K. Norskov, Angew. Chem. Int. Ed. 44 (2005) 1824.
[18] A. Rodriguez, S. Ma, P. Liu, J. Hrbek, J. Evans, M. Pérez, Science 318 (2007) 1757.
[19] Q. Fu, W. Deng, H. Saltsburg, M. Flytzani-Stephanopoulos, Appl. Catal. B: Environ. 56 (2005) 57.
[20] S. Ricote, G. Jacobs, M. Milling, Y.Y. Ji, P.M. Patterson, B.H. Davis, Appl. Catal. A: Gen. 303 (2006) 35.
[21] T. Bunluesin, R.J. Gorte, G.W. Graham, Appl. Catal. B: Environ. 15 (1998) 107.
[22] P. Liu, J.A. Rodriguez, J. Chem. Phys. 126 (2007) 164705.
[23] X. Wang, J.A. Rodriguez, J.C. Hanson, D. Gamarra, A. Martinez-Arias, M. Fernandez-Garcia, Top. Catal. 49 (2008) 81.
[24] J.A. Rodriguez, P. Liu, J. Hrbek, M. Pérez, J. Evans, J. Mol. Catal. A: Chem. 281 (2008) 59.
[25] J.A. Rodríguez, J. Evans, J. Graciani, J.-B. Park, P. Liu, J. Hrbek, J.F. Sanz, J. Phys. Chem. C 113 (2009) 7364.
[26] S.D. Senanayake, D. Stacchiola, P. Liu, C.B. Mullins, J. Hrbek, J.A. Rodriguez, J. Phys. Chem. C 113 (2009) 19536.
[27] S.D. Senanayake, D. Stacchiola, J. Evans, M. Estrella, L. Barrio-Pliego, M. Pérez, J. Hrbek, J.A. Rodríguez, J. Catal. 271 (2010) 392.
[28] J.A. Rodriguez, J. Hrbek, Surf. Sci. 604 (2010) 241.
[29] J.B. Park, J. Graciani, J. Evans, D. Stacchiola, S. Ma, P. Liu, A. Nambu, J.F. Sanz, J. Hrbek, J.A. Rodriguez, Proc. Natl. Acad. Sci. 106 (2009) 4975.
[30] I.D. Gonzalez, R.M. Navarro, W. Wen, N. Marinkovic, J.A. Rodríguez, F. Rosa, J.L.G. Fierro, Catal. Today 149 (2010) 372.
[31] V. Schwartz, D.R. Mullins, W. Yan, B. Chen, S. Dai, S.H. Overbury, J. Phys. Chem. B 108 (2004) 15782.
[32] C.T. Campbell, K. Daube, J. Catal. 104 (1987) 109.
[33] J. Nakamura, J.M. Campbell, C.T. Campbell, J. Chem. Soc., Faraday Trans. 86 (1990) 2725.
[34] R.A. Ojifinni, N.S. Froemming, J. Gong, M. Pan, T.S. Kim, J.M. White, G. Henkelman, C.B. Mullins, J. Am. Chem. Soc. 130 (2008) 6801.
[35] T.S. Kim, J. Gong, R.A. Ojifinni, J.M. White, C.B. Mullins, J. Am. Chem. Soc. 128 (2006) 6282.
[36] J.A. Rodriguez, J. Graciani, J. Evans, J.B. Park, F. Yang, D. Stacchiola, S.D. Senanayake, S. Ma, M. Perez, P. Liu, J. Fdez. Sanz, J. Hrbek, Angew. Chem. Int. Ed. 48 (2009) 8047.
[37] A.A. Gokhale, J.A. Dumesic, M. Mavrikakis, J. Am. Chem. Soc. 130 (2008) 1402.
[38] J.A. Rodriguez, D. Stacchiola, Phys. Chem. Chem. Phys, 2010, doi:10.1039/C003665J.
[39] H.H. Kung, Transition Metal Oxides: Surface Chemistry and Catalysis, Elsevier, Amsterdam, 1989.
[40] I.E. Wachs, Catal. Today 100 (2005) 79.
[41] J.A. Rodriguez, Theor. Chem. Acc. 107 (2002) 117.
[42] J.B. Park, J. Graciani, J. Evans, D. Stacchiola, S.D. Senanayake, L. Barrio, P. Liu, J.F. Sanz, J. Hrbek, J.A. Rodriguez, J. Am. Chem. Soc. 132 (2010) 356.
[43] M. Valden, X. Lai, D.W. Goodman, Science 281 (1998) 1647.
[44] J.L.C. Fajín, F. Illas, J.R.B. Gomes, J. Chem. Phys. 130 (2009) 224702.